Benzene Hydroxylation

DOI: 10.1002/anie.201105229

Electrochemical Oxidation of Benzene to Phenol**

*Byungik Lee, Hiroto Naito, and Takashi Hibino**

Phenol is an important intermediate for many products in the manufacture of resins, fibers, dyes, and medicines. Worldwide, the production of phenol is mostly conducted by the well-known cumene method, a three-step process that generates a large quantity of acetone as a by-product. To meet the increasing demand for phenol and to satisfy environmental-protection requirements, considerable efforts have been devoted to producing phenol by the one-step hydroxylation of benzene. The direct oxidation of benzene to phenol has been widely investigated with various oxidants, such as nitrous oxide,[1–4] hydrogen peroxide,[5–8] molecular oxygen,[9] and a mixture of hydrogen and oxygen.[10] Major issues concerning these processes are the deactivation of the catalyst by heavy coke formation in the gas-phase reaction[11] and separation of phenol from the reaction mixture in the liquid-phase reaction.[12]

As part of an alternative approach to the direct hydroxylation of benzene to phenol, the use of membrane reactors has been proposed because of their separation ability and operation under mild conditions. Niwa et al. reported that phenol was synthesized from benzene using a compact Pd membrane as a barrier permeable only to hydrogen and at the same time as a catalyst for the formation of active oxygen species.[13] A similar reactor was proposed based on a hydrogen-permeable PdCu membrane.[14] In general, however, the cost of such membrane materials is very high for industrial applications. In contrast, electrochemical membrane reactors offer a less expensive alternative to catalytic membrane reactors. Otsuka and Yamanaka et al., for example, showed the selective oxidation of benzene to phenol by an active oxygen species generated at the cathode in a phosphoric acid fuel cell [Reactions (1)–(3)].[15,16]

$$\text{Anode:}\quad H_2 \rightarrow 2\,H^+ + 2\,e^- \tag{1}$$

$$\text{Cathode:}\quad O_2 + 2\,H^+ + 2\,e^- \rightarrow O^* + H_2O \tag{2}$$

$$C_6H_6 + O^* \rightarrow C_6H_5OH \tag{3}$$

While phenol is the only product from benzene, the current efficiency for phenol production is merely 5.5%, because the predominant cathode reaction is not Reaction (2), but rather Reaction (4).

$$\text{Cathode:}\quad {}^1\!/_2\,O_2 + 2\,H^+ + 2\,e^- \rightarrow H_2O \tag{4}$$

One approach to overcoming this challenge of low efficiency is to generate an active oxygen species at the anode and then to oxidize benzene to phenol with the active oxygen species. We recently reported the partial oxidation of methane to methanol at V_2O_5-based anodes in the temperature range of 50–250°C, where the current efficiency for methanol production was as high as 61.4% at 100°C.[17] Therefore, if this process is applied to the direct hydroxylation of benzene to phenol, then phenol could be produced while maintaining high Faradaic efficiency [Reactions (5) and (6)].

$$\text{Anode:}\quad H_2O \rightarrow O^* + 2\,H^+ + 2\,e^- \tag{5}$$

$$C_6H_6 + O^* \rightarrow C_6H_5OH \tag{6}$$

In this case, the counter reaction at the cathode is Reaction (4).

Based on these observations and assumptions, it was expected that an electrochemical synthesis of phenol could be developed through Reactions (4)–(6). The goals of the present work were to: 1) enhance the current efficiency for phenol production by employing a more promising catalyst, and 2) clarify the reaction mechanism by various means, including electrochemical, kinetic, and spectroscopic techniques.

The electrochemical oxidation of benzene was first tested using various metal oxides (V_2O_5, Mn_2O_3, CoO, CuO, Fe_2O_3, MoO_3, MgO, WO_3, ZrO_2, and Cr_2O_3), some of which have been reported as being promising catalyst candidates for phenol production,[1–4,6,7,12,15] as the anode material at 50°C (see Table S1 in the Supporting Information). When a current of 1 mA was applied to the electrochemical cell, the production of phenol was observed over all the anode materials. Small quantities of CO_2 were also produced over the Mn_2O_3, CoO, MoO_3, MgO, and WO_3 anodes. Moreover, the production of phenol at the V_2O_5 anode was found to be the most significant among the anodes tested: the current efficiency for phenol production and selectivity toward phenol were 41.7 and 100%, respectively. Vanadium is one of the most widely used elements in catalysts for the direct hydroxylation of benzene to phenol with hydrogen peroxide.[18–20] Therefore, V_2O_5 was employed as the anode material in subsequent experiments.

Different oxidation currents were applied to the V_2O_5 anode in the temperature range of 25–100°C. Figure 1a shows the current as a function of anode potential. Although the anode potential at 0 mA was negative independent of temperature, the anode potential was significantly shifted to the positive side by an increase in the current, because of to the large internal electrical resistance of the electrochemical cell. It should also be kept in mind that a similar relationship between the anode potential and current was observed in the

---

[*] B. Lee, H. Naito, Dr. T. Hibino
Graduate School of Environmental Studies, Nagoya University
Furo-cho, Chikusa-ku, Nagoya 464-8601 (Japan)
E-mail: hibino@urban.env.nagoya-u.ac.jp

[**] This work was supported by KAKENHI (21350073).

Supporting information for this article is available on the WWW under http://dx.doi.org/10.1002/anie.201105229.

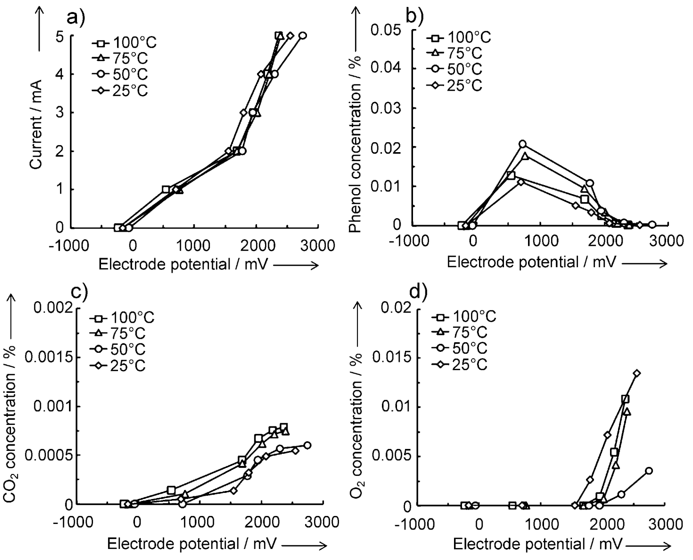

Figure 1. Electrochemical oxidation of benzene in the electrochemical cell from 25 to 100 °C. a) Current, b) phenol, c) CO_2, and d) O_2 concentrations as a function of anode potential.

temperature range tested, where the current suddenly increased at anode potentials around +1600 mV.

Next, the products in the outlet gas from the anode chamber at each temperature were analyzed. The results are shown in Figures 1 b,c, and d for phenol, CO_2, and O_2, respectively (other products were not detected in the analysis). Common features for the results obtained at all temperatures were that the phenol and CO_2 concentrations increased immediately upon application of current to the cell; and the phenol concentration initially increased and then decreased with increasing current, at which time the O_2 concentration started to increase. These results suggest that benzene is converted directly into phenol and CO_2 by means of Reaction (5) followed by Reactions (6) and (7), respectively, and O_2 is formed at high currents via Reaction (8).

$$\text{Anode}: \ 1/6\,C_6H_6 + 2\,O^* \rightarrow CO_2 + H^+ + e^- \tag{7}$$

$$2\,H_2O \rightarrow O_2 + 4\,H^+ + 4\,e^- \tag{8}$$

Interestingly, although the phenol concentration at each potential was dependent on the temperature, the production of phenol was always limited at anode potentials between +600 and +2000 mV (Figure 1 b), which suggests a close relationship between phenol production and the electrode potential. It is likely that formation of the active oxygen species for phenol production is inhibited by excess polarization of the anode, which results in the appearance of Reaction (8). For this reason, it is thought that a sudden increase in current occurs at potentials above +1600 mV (Figure 1 a). In any event, the optimal temperature for phenol production was determined to be 50 °C.

We conducted cyclic voltammetry (CV) measurements to understand the potential dependence of phenol production corresponding to Reactions (5) and (6). Figure 2 a shows an *I*–*V* curve of the anode in a gaseous mixture of benzene and H_2O at 50 °C, in addition to data recorded in the absence of benzene for comparison. A large anodic peak between +600 and +1800 mV was observed during anodic polarization in the presence of benzene, whereas such a peak did not appear in the absence of benzene. Therefore, this peak can be attributed to benzene oxidation by the active oxygen species. However, further anodic polarization oxidizes the active oxygen species to atomic or molecular oxygen, which is assumed to be inactive toward the partial oxidation of benzene. These results correspond well with those shown in Figure 1 b.

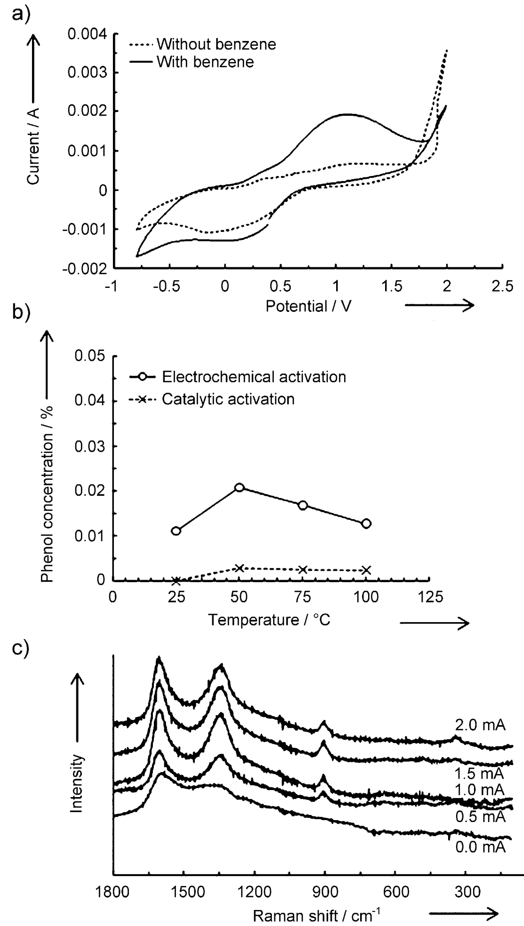

Figure 2. a) *I*–*V* profiles of the V_2O_5 anode with and without the presence of benzene at 50 °C. b) Phenol concentration over the V_2O_5 anode from 25 to 100 °C. This plot includes the result for the catalytic reaction between gaseous oxygen and benzene at the open-circuit voltage. c) Raman spectra of the surface of the V_2O_5 anode at room temperature. Constant currents were applied to the electrochemical cell in ambient atmosphere.

It would be useful to compare the electrochemical activation of oxygen with the catalytic activation of oxygen; therefore gaseous oxygen was added to the anode gas outside the system. An oxygen concentration of 0.01 vol % is equivalent to the amount of oxygen formed by passing a current of 1 mA through the electrochemical cell. The results of this comparison are shown in Figure 2 b. The concentrations of phenol produced with gas-phase oxygen at the open-circuit voltage (OCV) were found to be considerably lower than those obtained by applying a current of 1 mA. In particular, no phenol was produced with gas-phase oxygen at 25 °C. These results reflect the large difference in quality between the electrochemically and catalytically activated oxygen species.

Different active oxygen species, such as O, $HO^{\bullet}$, $HOO^{\bullet}$, O_2^{2-}, and O^-, have been proposed for phenol production.[4,13,21] To clarify which of these is the active oxygen species in the present study, Raman spectra from the surface of the V_2O_5 anode were measured during application of current to the electrochemical cell. As can be seen in Figure 2c, a band appears at 900 cm^{-1} when current is flowing, which is assigned to the OH bending mode.[22] It is thus reasonable to conclude that the active oxygen species for benzene oxidation is the $HO^{\bullet}$ radical. According to the reaction mechanism proposed by Miyahara et al.,[23] the following reaction scheme is possible, where (C_6H_6OH) is a hydroxycyclohexadienyl radical [Reactions (9) and (10)].

$$\text{Anode}: \; C_6H_6 + HO^{\bullet} \rightarrow (C_6H_6OH) \tag{9}$$

$$(C_6H_6OH) + V^{V} \rightarrow C_6H_5OH + H^+ + V^{IV} \tag{10}$$

Reaction (10) suggests that the reduced V^{IV} is required to be re-oxidized to V^{V}, which may be promoted by the presence of mixed-valence vanadium. An attempt was made to form such vanadium ions by reducing the V_2O_5 anode at elevated temperatures, and the resultant phenol, CO_2, and O_2 concentrations are shown in Figures 3 a, b, and c, respectively. The phenol concentration increased with increasing reduction temperature, reached a maximum at 400 °C, and then decreased for the reduction temperature of 450 °C. It is to be noted that there was almost no difference in current at each potential for all reduction temperatures (data not shown). As a result, the current efficiency for phenol production was significantly increased to 76.5 % with a high selectivity toward phenol of 94.7 % at the reduction temperature of 400 °C. Another important result is that the phenol concentration again reached a peak at potentials around +1000 mV for all reduction temperatures, which indicates the large effect of the electrode potential on phenol production.

To gain insight into the reaction site for phenol production on the reduced V_2O_5 anode, we characterized the electrode sample using X-ray diffraction (XRD) and X-ray photoelectron spectroscopy (XPS). Figure 4 a shows that peaks attributable to VO_2 appeared in the XRD patterns when the sample was reduced at 350 °C or higher, with the peak intensities being largest at 400 °C. Upon further increase in reduction temperature, peaks assigned to V_2O_3 were observed for the sample reduced at 450 °C. Considering the results shown in Figure 3 a together with the XRD data, it can be assumed that the presence of VO_2 plays an important role in thr formation of phenol. Indeed, the V $2p_{3/2}$ XPS spectrum, shown in Figure 4 b, had a small peak assigned to V^{4+} for the sample reduced at 400 °C. The concentration ratio of V^{4+}/(total V cations) estimated from the relative peak areas for the V $2p_{3/2}$ spectrum was 0.08.

Based on the above results, it is speculated that the reaction site for phenol production is either V^{4+} alone or a combination of V^{4+} and V^{5+}. The answer to this speculation is provided by comparing the activity of the pure VO_2 anode for phenol production with the results shown in Figure 3 a. The concentration of phenol produced over the VO_2 anode at 1 mA was 0.021 vol %, which is considerably less than the 0.038 vol % observed for the reduced V_2O_5 anode. This result strongly suggests that the reaction site can be assigned to a V^{4+}/V^{5+} redox pair. A similar conclusion was reached by Lemke et al., though they used hydrogen peroxide as an oxidant.[24] It is probable that Reaction (10) is promoted at the redox site in the present case.

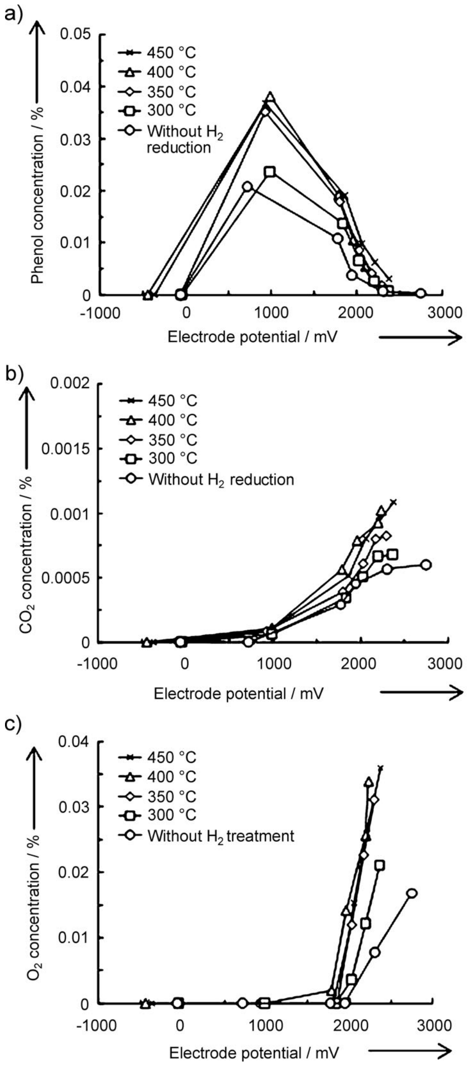

Figure 3. Product concentrations observed using the V_2O_5 anode reduced at different temperatures. a) Phenol, b) CO_2, and c) O_2 concentrations as a function of anode potential. The reaction temperature was 50 °C.

This study demonstrates that benzene can be oxidized directly to phenol in an electrochemical cell. Our emphasis is electrochemical oxidation of benzene to phenol at the anode, which yields a much higher Faradaic efficiency for phenol production than that for the electrochemical oxidation of benzene to phenol at the cathode. However, the phenol yield at present is substantially lower owing to the small area of the

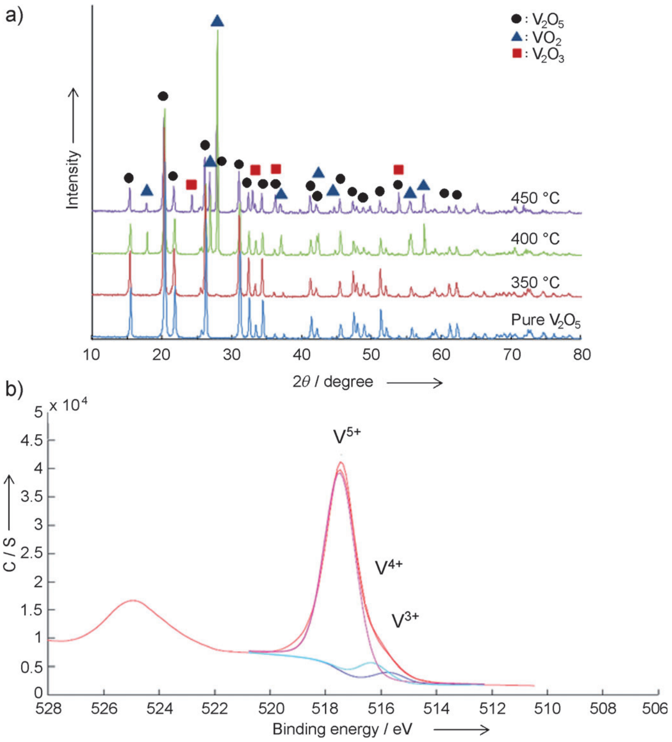

Figure 4. a) XRD patterns of the V_2O_5 anode reduced at different temperatures. b) XPS spectrum of the V_2O_5 anode reduced at 400 °C.

electrode used. This challenge can be overcome not only by scaling up the reactor system, but also by distributing the $Sn_{0.9}In_{0.1}P_2O_7$ ionomer over the V_2O_5 anode. In particular, since the latter drastically increases the number of reaction sites per unit area, it is an effective method for practical applications.

Experimental Section

Materials: Proton conductors are important materials for this study. The proton conductor used was $Sn_{0.9}In_{0.1}P_2O_7$ because this material displays a proton conductivity above 0.05 $S\,cm^{-1}$ in the temperature range of 50–300 °C.[25] SnO_2 and In_2O_3 were mixed with 85 % H_3PO_4 and de-ionized water. The mixture was stirred at 300 °C until it formed a high-viscosity paste. This paste was calcined in a covered alumina crucible at 650 °C for 2.5 h and then ground with a mortar and pestle. The characteristics of $Sn_{0.9}In_{0.1}P_2O_7$, including the electrochemical properties, crystalline structure, and composition, have been described elsewhere.[26]

Various metal oxides (V_2O_5, Mn_2O_3, CoO, CuO, Fe_2O_3, MoO_3, MgO, WO_3, ZrO_2, and Cr_2O_3) were used as anode materials for phenol production. In each case 0.15 g of the metal oxide was suspended in a mixed solution of appropriate quantities of polytetrafluoroethylene (PTFE) and glycerin using a Thinky AR-100 mixer. The suspension was coated on a Toray TGPH-090 gas-diffusion layer and then heated in an Ar flow at 150 °C for 2 h. After washing with ethanol and drying at 70 °C for 1 h, the electrode was finally heated in an Ar flow at 350 °C for 1 h or in 10 vol % H_2 flow (balance Ar) at different temperatures for 1 h. The loading of all the anode materials was kept at 26 $mg\,cm^{-2}$. A commercially available Pt/C cathode (Pt loading: 1 $mg\,cm^{-2}$) was obtained from BASF.

Characterization: Raman analysis of the anode surface was carried out by setting up an electrochemical cell, with a small quantity of carbon powder added to the anode material as an electrical collector, in a JASCO NRS-1000 spectrophotometer. Raman spectra were recorded during the application of a constant current to the electrochemical cell with visible (532 nm) laser excitation. All Raman measurements were conducted at room temperature in ambient atmosphere. The anode materials were further characterized by XRD and XPS. Powder diffraction patterns were measured using a Rigaku Miniflex II diffractometer with $Cu_{K\alpha}$ radiation ($\lambda = 1.5432$ Å) operated at 45 kV and 20 mA. XPS analysis was conducted using a VG Escallab 220i-XL instrument with an $Al_{K\alpha}$ (1486.6 eV) X-ray source. The photoemission angle was set at 45° to the sample surface.

Electrochemical studies: The $Sn_{0.9}In_{0.1}P_2O_7$ powder was pressed into pellets (12 × 1 mm) under a pressure of 200 MPa. The anode and cathode (area: 0.5 cm^2) were arranged on opposite faces of the electrolyte pellet. Two gas chambers were prepared by placing the cell assembly between two alumina tubes. The anode and cathode chambers were supplied with a gaseous mixture of 5 vol % benzene and 1 vol % H_2O (balance Ar) and air, respectively, at a flow rate of 30 $mL\,min^{-1}$. Constant current was applied to the electrochemical cell using a Hokuto Denko HA-501 galvanostat. The potential of the anode versus the cathode was recorded with a Hokuto Denko HE-101 electrometer. The outlet gas from the anode chamber was analyzed using two online gas chromatographs with Shimadzu GC-2014 flame-ionization and Varian CP-4900 thermal-conductivity detectors. The theoretical concentrations of phenol, CO_2, and O_2 products in the outlet gas from the anode chamber were calculated from Faraday's law based on two-, five-, and four-electron reactions, respectively (see the Supporting Information, in addition to the selectivity toward phenol and the current efficiency for phenol production). Further detailed characteristics of the anode were obtained using CV with 5 vol % benzene and 1 vol % H_2O (Ar balance) supplied to the anode at a flow rate of 30 $mL\,min^{-1}$. CV profiles were collected between −0.8 and +2.0 V at a scan rate of 3 $mV\,s^{-1}$ (Hokuto Denko, HZ-5000).

Received: July 26, 2011

Keywords: active oxygen species · benzene oxidation · electrochemistry · phenol synthesis

---

[1] V. I. Sobolev, A. S. Kharitonov, Ye. A. Paukshtis, *J. Mol. Catal.* **1993**, *84*, 117–124.
[2] R. Leanza, I. Rossetti, I. Mazzola, L. Forni, *Appl. Catal. A* **2001**, *205*, 93–99.
[3] J. Jia, K. S. Pillai, W. M. H. Sachetler, *J. Catal.* **2004**, *221*, 119–126.
[4] V. S. Chernyavsky, L. V. Pirutko, A. K. Uriarte, A. S. Kharitonov, G. I. Panov, *J. Catal.* **2007**, *245*, 466–469.
[5] J. Zhang, Y. Tang, G. Li, C. Hu, *Appl. Catal. A* **2005**, *278*, 251–261.
[6] Y. Zhong, G. Li, L. Zhu, Y. Yan, G. Wu, C. Hu, *J. Mol. Catal. A* **2007**, *272*, 169–173.
[7] S. Song, H. Yang, R. Rao, H. Liu, A. Zhang, *Appl. Catal. A* **2010**, *375*, 265–271.
[8] M. L. Neidig, K. F. Hirsekorn, *Catal. Commun.* **2011**, *12*, 480–484.
[9] Y. Liu, K. Murata, M. Inaba, *J. Mol. Catal. A* **2006**, *256*, 247–255.
[10] T. Miyake, M. Hamada, H. Niwa, M. Nishizuka, M. Oguri, *J. Mol. Catal. A* **2002**, *178*, 199–204.
[11] P. Zhai, L. Wang, C. Liu, S. Zhang, *Chem. Eng. J.* **2005**, *111*, 1–4.
[12] R. Molinari, T. Poerio, T. Granato, A. Katovic, *Microporous Mesoporous Mater.* **2010**, *129*, 136–143.
[13] a) S. Niwa, M. Eswaramoorthy, J. Nair, A. Raj, N. Itoh, H. Shoji, T. Namba, F. Mizukami, *Science* **2002**, *295*, 105–107; b) K. Sato, S. Hamakawa, M. Natsui, M. Nishioka, T. Inoue, F. Mizukami, *Catal. Today* **2010**, *156*, 276–281.

[14] R. Dittmeyer, L. Bortolotto, *Appl. Catal. A* **2011**, *391*, 311–318.

[15] a) K. Otsuka, I. Yamanaka, K. Hosokawa, *Nature* **1990**, *345*, 697–698; b) I. Yamanaka, T. Onizawa, S. Takenaka, K. Otsuka, *Angew. Chem.* **2003**, *115*, 3781–3783; *Angew. Chem. Int. Ed.* **2003**, *42*, 3653–3655.

[16] I. Yamanaka, T. Akimoto, K. Otsuka, *Electrochim. Acta* **1994**, *39*, 2545–2549.

[17] B. Lee, T. Hibino, *J. Catal.* **2011**, *279*, 233–240.

[18] X. Gao, J. Xu, *Appl. Clay Sci.* **2006**, *33*, 1–6.

[19] Y. Zhu, Y. Dong, L. Zhao, F. Yuan, *J. Mol. Catal. A* **2010**, *315*, 205–212.

[20] S. Song, S. Jiang, R. Rao, H. Yang, A. Zhang, *Appl. Catal. A* **2011**, *401*, 215–219.

[21] Y. Moro-oka, M. Akita, *Catal. Today* **1998**, *41*, 327–338.

[22] L. D. Nguyen, S. Loridant, H. Launay, A. Pigamo, J. L. Dubois, J. M. M. Millet, *J. Catal.* **2006**, *237*, 38–48.

[23] T. Miyahara, H. Kanzaki, R. Hamada, S. Kuroiwa, S. Nishiyama, S. Tsuruya, *J. Mol. Catal. A* **2001**, *176*, 141–150.

[24] K. Lemke, H. Ehrich, U. Lohse, H. Berndt, K. Jähnisch, *Appl. Catal. A* **2003**, *243*, 41–51.

[25] M. Nagao, A. Takeuchi, P. Heo, T. Hibino, M. Sano, A. Tomita, *Electrochem. Solid-State Lett.* **2006**, *9*, A105–A109.

[26] Y. C. Jin, Y. B. Shen, T. Hibino, *J. Mater. Chem.* **2010**, *20*, 6214–6217.